Published in final edited form as:
Heart Rhythm. 2011 March ; 8(3): 448–454. doi:10.1016/j.hrthm.2010.11.019.

Morphologic pattern of the intrinsic ganglionated nerve plexus in the mouse heart

Kristina Rysevaite[1], **Inga Saburkina**[1], **Neringa Pauziene**[1], **Sami Noujaim**[2], **José Jalife**[2], and **Dainius H. Pauza**[1,*]

[1]Institute of Anatomy, Kaunas University of Medicine, Lithuania

[2]Center for Arrhythmia Research, University of Michigan, USA

Summary

BACKGROUND—Both normal and genetically modified mice are excellent models to investigate molecular mechanisms of arrhythmogenic cardiac diseases that may associate with an imbalance between the sympathetic and the parasympathetic nervous input to the heart.

OBJECTIVE—We sought to: (1) determine the structural organization of the mouse cardiac neural plexus; (2) identify extrinsic neural sources and their relationship with the cardiac plexus; and (3) reveal any anatomical differences in the cardiac plexus between mouse and other species.

METHODS—Cardiac nerve structures were visualized employing histochemical staining for acetylcholinesterase (AChE) on whole heart and thorax-dissected preparations derived from 25 mice. To confirm reliability of staining parasympathetic and sympathetic neural components in the mouse heart we applied a histochemical method for AChE and imunohistochemistry for tyrosine hydroxylase (TH) and/or choline acetyltransferase (ChAT) on whole mounts preparations from 6 mice.

RESULTS—The double immunohistochemical labeling of TH and ChAT on AChE positive neural elements in mouse whole mounts demonstrated equal staining of nerves and ganglia for AChE that were positive for both TH and ChAT. The extrinsic cardiac nerves access the mouse heart at the right (RCV) and left (LCV) cranial veins and interblend within the ganglionated nerve plexus of the heart hilum that is persistently localized on the heart base. Nerves and bundles of nerve fibers extend epicardially from this plexus to atria and ventricles by left dorsal, dorsal right atrial, right ventral, and ventral left atrial routes or subplexuses. The RCV received extrinsic nerves mainly originated from the right cervicothoracic ganglion and a branch of the right vagus nerve, while the LCV was supplied by extrinsic nerves from the left cervicothoracic ganglion and the left vagus nerve. The majority of intrinsic cardiac ganglia were localized on the heart base at the roots of pulmonary veins. These ganglia were interlinked by interganglionic nerves into the above mentioned nerve plexus of the heart hilum. In general, the examined hearts contained 19 ± 3 ganglia, which gave a cumulative ganglion area of 0.4 ± 0.1 mm^2.

CONCLUSION—Despite substantial anatomical differences in ganglion number and distribution, the structural organization of the intrinsic ganglionated plexus in the mouse heart corresponds in general to other mammalian species, including human.

*Correspondence to: Prof. Dainius H. Pauza, Institute for Anatomy, Faculty of Medicine, Lithuanian University of Health Sciences, A. Mickeviciaus Street 9, Kaunas LT-44307, Lithuania. dainius.pauza@kmu.lt; Phone: +370 37 327313; Fax: +370 37 220733; Mobile: + 370 682 39366.

No Conflicts

Keywords

Intrinsic cardiac neural plexus; ganglia; neurons; acetylcholinesterase; choline acetyltransferase; tyrosine hydroxylase; heart; mouse

Introduction

The intrinsic cardiac nervous system plays a crucial role in the regulation of the heart rate and atrioventricular nodal conduction, as well as atrial and ventricular inotropism[1–3]. It has been proposed that cardiac parasympathetic neurons from the dorsal motor nucleus and the nucleus ambiguous project their axons to the intrinsic cardiac neurons and that the neurons from the dorsal motor nucleus regulate cardiac inotropism, while those in the nucleus ambiguous are related to heart rate control[4,5]. Preganglionic sympathetic axons from neurons in the T1-T5 spinal segments project to secondary sympathetic neurons that are located in the sympathetic chain, as well as the mediastinal and intrinsic cardiac ganglia[5–7]. The sensory neurons associated with cardiac function have been identified inside the nodose, C1-T4 dorsal root, mediastinal and intrinsic cardiac ganglia[5,6,8,9]. Recent findings suggest that intrinsic sensory cardiac neurons are also involved in local neural circuits via their axonal projections to efferent neurons distributed within the same or neighboring intrinsic ganglia[5]. Possibly, this diversity of neurons composes an integrative neuronal network, which modulates extrinsic autonomic projections to the heart and mediates local cardiac reflexes[10]. In addition, the integrative function of the intrinsic cardiac neurons is under the tonic influence of neurons from the insular cortex, brainstem and spinal cord[5,10,11].

Morphologically, the intrinsic cardiac nervous system corresponds to the neural ganglionated plexus, which has been subdivided according to the layers of the heart wall into epicardial, myocardial and endocardial[12]. Recent neuroanatomical investigations have demonstrated that the intrinsic cardiac neural plexus may be considered as a complex of distinct ganglionated subplexuses. Intrinsic ganglia related to particular subplexuses are distributed at specific atrial or ventricular regions around the sinuatrial node, the roots of caval and pulmonary veins, and near the atrioventricular node[13–15].

The recent elucidation of the complete mouse genome in combination with transgenesis and gene targeting in embryonic stem cells have opened excellent opportunities for modeling and investigating molecular mechanisms of the role of sympathetic-parasympathetic imbalance in cardiac arrhythmia predisposition[16,17]. However, the neuroanatomy of the mouse heart has been the subject of very few investigations to this date[18,19]. Therefore, we sought to: (1) determine the structural organization of the mouse cardiac neural plexus; (2) identify extrinsic neural sources and their relationship with the cardiac plexus; and (3) reveal anatomical differences between the mouse cardiac plexus and those of other species in order to validate neuroanatomically the mouse model for its exploitation in experimental cardiac arrhythmia research.

Materials and Methods

Thirty one adult C57BL/6J-linear mice of both sexes were obtained from the Animal Center of the Institute of Immunology (Vilnius, Lithuania). Animals were in accordance with local and state guidelines for the care and use of experimental animals. The animals were deeply anesthetized with diethyl ether and euthanized by cervical dislocation.

PREPARATIONS

TOTAL HEART PREPARATIONS—After thoracotomy, the mouse body was perfused with 0.01 M phosphate buffered saline (PBS), consisting of 8.06 mM Na_2HPO_4, 1.94 mM NaH_2PO_4, and 137 mM NaCl in high purity distilled H_2O (pH 7.4), at room temperature. In order to stain the nerve plexus in whole, i.e. non-parceled and non-sectioned, mouse heart, fifteen mouse hearts were prepared for histochemical acetylcholinesterase (AChE) staining, as described previously[20]. The flabby atrial walls were distended *in situ* via transmyocardial injection of a 20% warm water solution of gelatin into the atria and ventricles. Once the injected gelatin jelled, the heart was removed from the chest and immersed in a chamber filled with room temperature PBS. Subsequently, the remains of the pericardium, pulmonary arteries and mediastinal fat were gently separated from the heart base. The prepared hearts were prefixed for 30 min at 4°C in 4% paraformaldehyde solution in 0.01 M phosphate buffer (pH 7.4). After prefixation, the heart preparations were washed for 12 hours at 4°C in PBS containing hyaluronidase (0,5 mg/100 ml, SERVA, Heidelberg, Germany) and placed for 3 hours at 4°C in Karnovsky-Roots medium as described previously[20]. Finally, heart reparations stained for AChE were fixed and stored in 4% paraformaldehyde solution in 0.01 M phosphate buffer (pH 7.4).

THORAX-DISSECTED PREPARATIONS—We microdissected ten mouse chests to stain the vagal nerves, the sympathetic chains, their ganglia and the branches linked macroanatomically to the intrinsic cardiac nerve ganglionated plexus. After perfusing PBS at room temperature and injecting 20% warm water solution of gelatin into the heart and great vessels, the anterior and lateral walls of the chest cavity were carefully dissected out at the rib necks, and the vertebral column was cut out at the twelfth thoracic vertebra. The thorax-dissected preparations were placed into a chamber filled with room temperature PBS, where lungs, pericardium and pulmonary arteries were carefully separated from the heart base. Vagal and sympathetic chain nerves of both sides and their branches extending toward the heart were microdissected using a Stemi 200 CS stereoscopic microscope (ZEISS, Gottingen, Germany) at 12.5× magnification. The prepared thorax-dissected preparations were fixed, washed, stained histochemically for AChE and stored according to the protocol described above.

WHOLE-MOUNT PREPARATIONS—To determine whether both types of efferent nerve fibers and ganglion cells were visualized by the above described histochemical method for acetylcholinesterase, double labeling for tyrosine hydroxylase (TH) and choline acetyltransferase (ChAT) was performed on six whole-mount murine heart preparations. After perfusion with PBS at room temperature, hearts were removed from the chest and placed into a dissecting dish containing PBS. The walls of the atria and interatrial septum were separated from the ventricles, then the septum was trimmed free of the atrial walls, and the atrial tissue was pinned flat on the dissecting dish. Tissue was fixed for 25 min at 4°C in 4% paraformaldehyde solution in 0.01 M phosphate buffer (pH = 7.4). To decrease background light during fluorescent microscopy, the tissues were cleared using a dimethyl sulfoxide and hydrogen peroxide solution, and dehydrated as reported previously[21]. After tissue clearing, the whole-mount preparations were rehydrated with 10 min successive washes through a graded ethanol series, washed and permeabilized in 3 × 10 min changes of 0.01 M PBS, containing 0.5% Triton X–100 (Serva, Heidelberg, Germany). The non–specific binding was blocked for 2 hours in PBS containing 5% normal donkey serum (Jackson ImmunoResearch Laboratories, West Grove, PA, USA), and 0.5% Triton X–100. After this, specimens were washed in 0.01 M PBS and covered by a large drop of a mixture of goat polyclonal anti-ChAT (dilution 1:100; AB144P, Chemicon, Millipore Corp., Billerica, MA, USA) antibody and rabbit polyclonal anti–TH (dilution 1:500, AB152, Chemicon, Millipore Corp., Billerica, MA, USA) antibody to label, respectively, the

cholinergic and adrenergic nerve fibers and cells. Incubation with primary antibodies persisted for 48 hours in a humid chamber at 4° C. Afterward, whole mounts were washed 3 times for 10 min in 0.01 M PBS and placed in a mixture of species-specific donkey secondary antibodies conjugated with Cy3 (dilution 1:400, AP180C, Chemicon, Millipore Corp., Billerica, MA, USA) and FITC (dilution 1:150, AP182F, Chemicon, Millipore Corp., Billerica, MA, USA) for 4 hours at room temperature. Later, specimens were washed 3 times for 10 min in 0.01 M PBS, cleared for one hour in a solution of dimethylsulfoxide and PBS (1:4 v/v), mounted with a Vectorshield Mounting Medium (Vector Laboratories, Inc., Burlingame, CA, USA) and cover slipped.

MICROSCOPIC EXAMINATION AND QUANTITATIVE ANALYSIS

The neural structures visualized histochemically for AChE were examined stereoscopically at 12.5× magnification using a Stemi 200 CS stereomicroscope (Zeiss, Gottingen, Germany) applying a transient light from optic fiber illuminators (Zeiss, Gottingen, Germany). To identify the external morphology of certain ganglia and the number of interganglionic nerves, preparations were additionally analyzed using a contact microscope LUMAM K-1 (Lomo, St Petersburg, Russia) at 10× magnification. The stereoscopically observed ganglia and nerves were photographed at 4× using an objective Microplanar (F = 65 mm; Lomo, St Petersburg, Russia) and digital camera Axiocam HRc (Zeiss, Gottingen, Germany). The adjustments of final images and measurements of cardiac ganglia were performed using AxioVision 4.7.1 software (Zeiss, Jena, Germany). The whole mounts stained immunohistochemically were analyzed utilizing an AxioImager Z1 fluorescence microscope (Zeiss, Gottingen, Germany) equipped with a set of filters to observe the fluorescein isothiocyanate (FITC) and cyanine (Cy3) fluorescence, an Apotome (Zeiss, Gottingen, Germany), optics for a differential interferential contrast (DIC) and digital monochrome camera AxioCam MRm (Zeiss, Gottingen, Germany).

STATISTICAL ANALYSIS

Data were expressed as mean ± standard error of the mean (SEM). Linear regression was used to quantitatively estimate the relation between the ganglion area and the number of interganglionic nerves (Microcal Origin 6.1, Microcal Software Inc., Northampton, MA, USA). Significance was accepted at $P < 0.05$.

Results

DISTRIBUTION OF TH- AND CHAT-STAINED NERVE FIBERS IN THE INTRINSIC CARDIAC NERVES

Immunohistochemistry for TH and ChAT performed after histochemical staining of intrinsic cardiac nerves and ganglia for AChE (see Methods) demonstrated clearly the coincident AChE distribution with both the TH and ChAT positive nerve fibers (Fig. 1). Although AChE positivity or intensity of staining was not precisely measured in this study, it was obvious that intraneural staining for AChE occurs even in nerves that involve principally the TH immunoreactive nerve fibers (Fig. 1). In general, the ChAT immunoreactive nerve fibers did prevail in comparatively thinner epicardial nerves that were the most intensely stained by brown precipitates of histochemical reaction for AChE. All intrinsic cardiac ganglia examined in the present study contained the ChAT immunoreactive neurons and were well stained for AChE.

ACCESS OF MEDIASTINAL NERVES INTO THE MOUSE HEART

The left and right cervicothoracic and the second thoracic sympathetic ganglia as well the both vagal nerves were obvious neural sources from which extrinsic nerves extended toward

and reached the mouse heart hilum. The right sympathetic and vagal nerves got into the heart hilum at the right cranial vein, whereas the left nerves entered at the left cranial vein (Fig. 2–4).

ARCHITECTURE AND TOPOGRAPHY OF THE INTRINSIC CARDIAC NERVE PLEXUS

At the limit of the venous portion of the heart hilum, beneath the bifurcation of the pulmonary trunk and within fatty connective tissue, the extrinsic cardiac nerves form a ganglionated nervous plexus that consistently contains right and left atrial clusters of ganglia (Figs 2–4). The right-sided nerves enter the ganglionic cluster located on the right atrium at the RCV on the ventral and cranial aspects of the interatrial groove (Figs 2 and 3d). From these ganglia, epicardial nerves spread mainly onto the ventral, dorsal and lateral surfaces of the right atrium which we have termed, respectively, the right ventral and dorsal right atrial neural pathways or nerve subplexuses (Figs 2; 3d; 4). The right ganglionic cluster supplies presumably the interatrial septum as some fine nerves derived from these ganglia penetrated into dorsal aspect of interatrial septum (Fig. 3a). The left-sided nerves access the left atrial ganglionic cluster at the LCV and from them epicardial nerves proceed onto (1) the ventral surface of the left atrium as the ventral left atrial neural pathway; and (2) the dorsal surfaces of the left atrium and both ventricles as the left dorsal neural pathway or subplexus (Figs 2a; 3a; 4). In all examined preparations, the vast majority of the ventral left atrial subplexal nerves made consistent anastomoses with the right ventral subplexal nerves on the ventral aspect of the interatrial groove (Fig. 2a). In the heart illustrated in Fig. 2a, both right and left atrial ganglionic clusters intercommunicated by thin commissural nerves. Similarly to some fine nerves derived from the right ganglionic cluster, a few nerves derived from the left dorsal neural subplexus extended towards and penetrated into the dorsal aspect of interatrial septum as well (Fig. 3a). Moreover, sparse extrinsic cardiac nerves attaining the mouse heart through the arterial part of the heart hilum extended directly into the epicardium of the ventricles. In all examined hearts, these nerves passed between the roots of the aorta and the pulmonary trunk, were not ganglionated and passed along the anterior interventricular groove as the left coronary neural pathway (Figs 2d and 4).

The distribution of cardiac nerves and the number of ganglia in whole heart as well as in separate subplexuses varied substantially from heart to heart (Fig. 5).

MORPHOLOGY OF THE MURINE CARDIAC GANGLIA

Intrinsic ganglia in the mouse heart varied significantly in appearance, but the majority of them were oval in shape (Figs 2 and 3). The size of these ganglia was extremely variable and ranged from those that were poorly observable with a dissecting microscope to ganglia that were discernible with the naked eye (Table 1). Multifold variability was characteristic for both the cumulative ganglion area and the number of cardiac ganglia (Table 1). Usually, nerve cells inside a ganglion were densely packed in 2–3 cell layers, but certain ganglia contained neurons bedded in 4–5 cell layers (Figs 2b, c; 3b, d). Numerous interganglionic nerves interlinked the mouse cardiac ganglia (Table 1; Fig. 2a). Evidently, the large ganglia possessed more interganglionic nerves than the small ones (Figs 2b, c; 3b, c). In fact, there was a strong correlation between the number of interganglionic nerves and the cardiac ganglion area (Fig. 6).

Discussion

This is the first detailed investigation of the anatomy of the intrinsic ganglionated nerve plexus of the whole, i.e. non-parceled and non-sectioned, mouse heart. Our study revealed the intrinsic ganglionated nerve plexus by using histochemical staining for AChE that has been considered by some investigators as a specific method to visualize exceptionally the

parasympathetic neural structures[22–26]. The simultaneous histochemical staining for AChE and immunohistochemical staining for TH and ChAT performed in the present study confirmed earlier findings by Koelle et al.[27] who demonstrated that AChE histochemistry according to Karnovsky and Roots[28] stains both sympathetic and parasympathetic neurons and nerves. Therefore there is no doubt that both parasympathetic and sympathetic neural structures were clearly visualized in this investigation employing the AChE histochemistry according to Karnovsky and Roots[28]. Nonetheless, it has been reported that sensory and postganglionic sympathetic nerve fibers have less AChE activity than cholinergic fibers[27,29]. Moreover, recent findings indicate the presence of multiple neurochemical phenotypes of mammalian cardiac neurons. For example, a dual cholinergic/nitrergic phenotype for intrinsic cardiac neurons[30], adrenergic/cholinergic phenotype for cardiac sympathetic neurons[16,31] and a co-transmission of acetylcholine, norepinephrine and NPY in sympathetic neurons co-cultured with target cardiac myocytes[31] has been recently demonstrated. Consequently, the lighter or weaker staining of some intrinsic cardiac nerves by AChE histochemical reaction products indicates presumably the predominance of non-cholinergic nerve fibers within those intrinsic cardiac nerves.

In our previous reports using hearts from humans, dogs, pigs, guinea pigs, rats and sheep, the intrinsic nerve plexus was analyzed as a complex of seven ganglionated nerve subplexuses, each of which threaded into the heart at a particular site of the heart hilum, occupied a specific location on the epicardium, extended to a restricted cardiac region, and included its own ganglionated field, preganglionated and postganglionated nerves[13,15,20,29,32,33]. Here we demonstrate that the structural organization of the mouse intrinsic nerve plexus is similar to those of other mammals. However, the particular intrinsic ganglionated nerve plexus of the heart hilum (GNPHH) is distributed on the base of the mouse heart and its postganglionated nerves extend toward both atria and ventricles. The preganglionated nerves access the GNPHH at both the right and the left cranial veins and join two ganglionic clusters interconnected by interganglionic nerves into a ring or chain of ganglia that in addition are interlinked by commissural nerves on the base of the left atrium. In general, the morphologic pattern of the mouse epicardial ganglionated nerve plexus is similar to, but somewhat less complex and dense than those of larger mammals, which accords to the small size of the mouse heart.

Sources of extrinsic cardiac nerves in the mouse heart are also rather distinct from those that were identified in humans, apes and sheep[7,29,34]. Preparations in this study revealed complete symmetry of the sympathetic and vagal sources, while in humans and sheep the left and right sympathetic and vagal cardiac nerves overlap in front of the heart and the left and right nerves access the heart in the same locations[7,29].

Employing a whole-mount preparation technique separately for each atrium of the mouse heart, Ai et al.[19] identified three discrete ganglionated plexuses that were distributed, respectively, at: (1) the entrance of the right pulmonary vein to the left atrium, and the junction of the right cranial vein and right atrium; (2) the entrance of the left cranial and caudal veins to the right atrium; and (3) the junction of the left pulmonary vein and the left atrium. Contrary to that report, our observations indicate that nerves extend to both atria and ventricles from the entire GNPHH by distinct nerve pathways of subplexuses. Moreover, some cardiac nerves reach the epicardium of the left ventricle directly through the arterial part of the HH. With respect to the distribution of the mouse cardiac ganglia, our findings are also in contradiction with the report of Ai et al.[19], in which intrinsic ganglia distributed in the region of sinuatrial node were mentioned. The present study does not confirm location of any ganglia above of the terminal groove in the typical region of the sinuatrial node. As is evident in Fig.4, the most ganglia revealed in this study were distributed in a distance from both the typical SA and AV nodes on the heart base.

Comparing the present observations with our earlier results in rat hearts[32], it is evident that the architecture and topography of the GNPHH in mice and rats are rather similar. In both species, the GPNHH ganglia are concentrated almost at the same locations. Also in both species, the epicardial nerves derived from the GNPHH extend topographically and morphologically following analogous routes and supply nearly identical atrial and ventricular regions. The most remarkable difference between mice and rats is in the nerve supply of the ventral surface of both ventricles. In rats, abundant nerves extend to the ventral surface of both ventricles from the arterial part of the heart hilum; i.e. they access the heart at the roots of the ascending aorta and pulmonary trunk[32]. In mice, the main nerve supply of the ventral surface of both ventricles is the right ventral pathway that gets underway from the right atrial cluster of ganglia in the GNPHH.

The present findings suggest that in general the topography and morphologic pattern of neural extensions from the mouse ganglionated nerve plexus of the heart hilum correspond to ganglionated nerve subplexuses in the human heart and this correspondence substantiates the usage of the mouse as a simple and reliable model in cardiac arrhythmia research. Hopefully, the neuroanatomy of the mouse heart demonstrated in this pilot study will facilitate further more advanced investigations with this animal model toward increasing knowledge of the physiological roles of distinct nerve pathways and individual intrinsic ganglia

Acknowledgments

The authors sincerely thank Mrs. Rima Masiene for technical assistance throughout the study. This work was in part supported by grant (No. PAR-18) from the Science Foundation of Kaunas University of Medicine and by NHLBI Grants P01-HL039707, P01-HL087226 and R01-HL080159 (JJ).

References

1. Gorman MW, Tune JD, Richmond KN, Feigl EO. Quantitative analysis of feedforward sympathetic coronary vasodilation in exercising dogs. J Appl Physiol. 2000; 89:1903–1911. [PubMed: 11053342]
2. Tsuboi M, Furukawa Y, Nakajima K, Kurogouchi F, Chiba S. Inotropic, chronotropic, and dromotropic effects mediated via parasympathetic ganglia in the dog heart. Am J Physiol Heart Circ Physiol. 2000; 279:H1201–H1207. [PubMed: 10993785]
3. Cifelli C, Rose RA, Zhang H, et al. RGS4 regulates parasympathetic signaling and heart rate control in the sinoatrial node. Circ Res. 2008; 103:527–535. [PubMed: 18658048]
4. Gatti PJ, Johnson TA, Phan P, Jordan IK 3rd, Coleman W, Massari VJ. The physiological and anatomical demonstration of functionally selective parasympathetic ganglia located in discrete fat pads on the feline myocardium. J Auton Nerv Syst. 1995; 51:255–259. [PubMed: 7769158]
5. Armour JA. Potential clinical relevance of the 'little brain' on the mammalian heart. Exp Physiol. 2008; 93:165–176. [PubMed: 17981929]
6. Horackova M, Armour JA, Byczko Z. Distribution of intrinsic cardiac neurons in whole-mount guinea pig atria identified by multiple neurochemical coding. A confocal microscope study. Cell Tissue Res. 1999; 297:409–421. [PubMed: 10460488]
7. Kawashima T. The autonomic nervous system of the human heart with special reference to its origin, course, and peripheral distribution. Anat Embryol (Berl). 2005; 209:425–438. [PubMed: 15887046]
8. Hopkins DA, Armour JA. Ganglionic distribution of afferent neurons innervating the canine heart and cardiopulmonary nerves. J Auton Nerv Syst. 1989; 26:213–222. [PubMed: 2754177]
9. Foreman RD. Neurological mechanisms of chest pain and cardiac disease. Cleve Clin J Med. 2007; 74 Suppl 1:S30–S33. [PubMed: 17455540]
10. Ardell, JL. Structure and function of mammalian intrinsic cardiac neurons. In: Armour, JA.; Ardell, JL., editors. Neurocardiology. New York: Oxford University Press; 1994. p. 95-114.

11. Oppenheimer, SM.; Hopkins, DA. Suprabulbar neuronal regulation of the heart. In: Armour, JA.; Ardell, JL., editors. Neurocardiology. New York: Oxford University Press; 1994. p. 309-342.
12. Marron K, Wharton J, Sheppard MN, et al. Distribution, morphology, and neurochemistry of endocardial and epicardial nerve terminal arborizations in the human heart. Circulation. 1995; 92:2343–2351. [PubMed: 7554220]
13. Pauza DH, Skripka V, Pauziene N. Morphology of the intrinsic cardiac nervous system in the dog: a whole-mount study employing histochemical staining with acetylcholinesterase. Cells Tissues Organs. 2002; 172:297–320. [PubMed: 12566631]
14. Arora RC, Waldmann M, Hopkins DA, Armour JA. Porcine intrinsic cardiac ganglia. Anat Rec A Discov Mol Cell Evol Biol. 2003; 271:249–258. [PubMed: 12552641]
15. Batulevicius D, Skripka V, Pauziene N, Pauza DH. Topography of the porcine epicardiac nerve plexus as revealed by histochemistry for acetylcholinesterase. Auton Neurosci. 2008; 138:64–75. [PubMed: 18063424]
16. Kanazawa H, Ieda M, Kimura K, et al. Heart failure causes cholinergic transdifferentiation of cardiac sympathetic nerves via gp130-signaling cytokines in rodents. J Clin Invest. 2010; 120:408–421. [PubMed: 20051627]
17. Koentgen F, Suess G, Naf D. Engineering the mouse genome to model human disease for drug discovery. Methods Mol Biol. 2010; 602:55–77. [PubMed: 20012392]
18. Maifrino LB, Liberti EA, Castelucci P, De Souza RR. NADPH- diaphorase positive cardiac neurons in the atria of mice. A morphoquantitative study. BMC Neurosci. 2006; 7:10. [PubMed: 16451738]
19. Ai J, Epstein PN, Gozal D, Yang B, Wurster R, Cheng ZJ. Morphology and topography of nucleus ambiguus projections to cardiac ganglia in rats and mice. Neuroscience. 2007; 149:845–860. [PubMed: 17942236]
20. Pauza DH, Skripka V, Pauziene N, Stropus R. Morphology, distribution, and variability of the epicardiac neural ganglionated subplexuses in the human heart. Anat Rec. 2000; 259:353–382. [PubMed: 10903529]
21. Dickie R, Bachoo RM, Rupnick MA, et al. Three-dimensional visualization of microvessel architecture of whole-mount tissue by confocal microscopy. Microvasc Res. 2006; 72:20–26. [PubMed: 16806289]
22. Crick SJ, Sheppard MN, Anderson RH, Polak JM, Wharton J. A quantitative study of nerve distribution in the conduction system of the guinea pig heart. J Anat. 1996; 188(Pt 2):403–416. [PubMed: 8621340]
23. Crick SJ, Sheppard MN, Ho SY, Anderson RH. Localisation and quantitation of autonomic innervation in the porcine heart I: conduction system. J Anat. 1999; 195(Pt 3):341–357. [PubMed: 10580850]
24. Kawano H, Okada R, Yano K. Histological study on the distribution of autonomic nerves in the human heart. Heart Vessels. 2003; 18:32–39. [PubMed: 12644879]
25. Hoover DB, Ganote CE, Ferguson SM, Blakely RD, Parsons RL. Localization of cholinergic innervation in guinea pig heart by immunohistochemistry for high-affinity choline transporters. Cardiovasc Res. 2004; 62:112–121. [PubMed: 15023558]
26. Otake H, Suzuki H, Honda T, Maruyama Y. Influences of autonomic nervous system on atrial arrhythmogenic substrates and the incidence of atrial fibrillation in diabetic heart. Int Heart J. 2009; 50:627–641. [PubMed: 19809211]
27. Koelle GB, Massoulie J, Eugene D, Melone MA, Boulla G. Distributions of molecular forms of acetylcholinesterase and butyrylcholinesterase in nervous tissue of the cat. Proc Natl Acad Sci U S A. 1987; 84:7749–7752. [PubMed: 3478723]
28. Karnovsky MJ, Roots L. A "Direct-Coloring" Thiocholine Method for Cholinesterases. J Histochem Cytochem. 1964; 12:219–221. [PubMed: 14187330]
29. Saburkina I, Rysevaite K, Pauziene N, et al. The Epicardial Neural Ganglionated Plexus of the Ovine Heart: Anatomical Basis for Experimental Cardiac Electrophysiology and Nerve Protective Cardiac Surgery. Heart Rhythm. 2010; 7:942–950. [PubMed: 20197118]

30. Hoover DB, Isaacs ER, Jacques F, Hoard JL, Page P, Armour JA. Localization of multiple neurotransmitters in surgically derived specimens of human atrial ganglia. Neuroscience. 2009; 164:1170–1179. [PubMed: 19747529]

31. A V, Ja L, Sj B, Ma M. Segregation of the classical transmitters norepinephrine and acetylcholine and the neuropeptide Y in sympathetic neurons: Modulation by CNTF or prolonged growth in culture. Dev Neurobiol. 2010 (Epub ahead of print).

32. Batulevicius D, Pauziene N, Pauza DH. Topographic morphology and age-related analysis of the neuronal number of the rat intracardiac nerve plexus. Ann Anat. 2003; 185:449–459. [PubMed: 14575272]

33. Batulevicius D, Pauziene N, Pauza DH. Architecture and age-related analysis of the neuronal number of the guinea pig intrinsic cardiac nerve plexus. Ann Anat. 2005; 187:225–243. [PubMed: 16130822]

34. Kawashima T, Thorington RW Jr. Kunimatsu Y, Whatton JF. Systematic morphology and evolutionary anatomy of the autonomic cardiac nervous system in the lesser apes, gibbons (hylobatidae). Anat Rec (Hoboken). 2008; 291:939–959. [PubMed: 18449901]

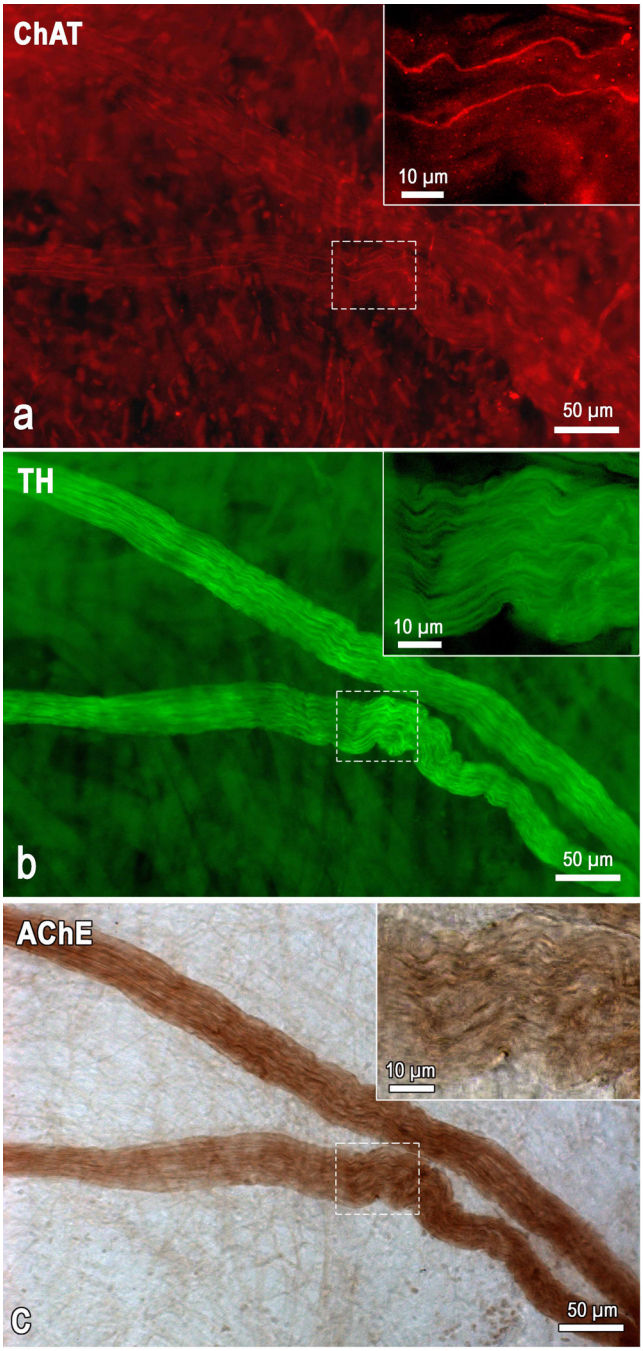

Fig 1.

Microphotograph demonstrating the presence of AChE within intrinsic cardiac nerves composed predominantly by TH-positive (adrenergic) and a few of ChAT-positive (cholinergic) nerve fibers. The image was taken from a whole mount heart preparation that was immunohistochemically double labeled for ChAT (a) and TH (b) and subsequently stained histochemically for AChE (c). Note the sharp contrast of the AChE staining compared with the ChAT labeling. Boxed areas within images were enlarged as the right upper insets to demonstrate the appearance of cholinergic and adrenergic nerve fibers within AChE positive nerve of mouse heart.

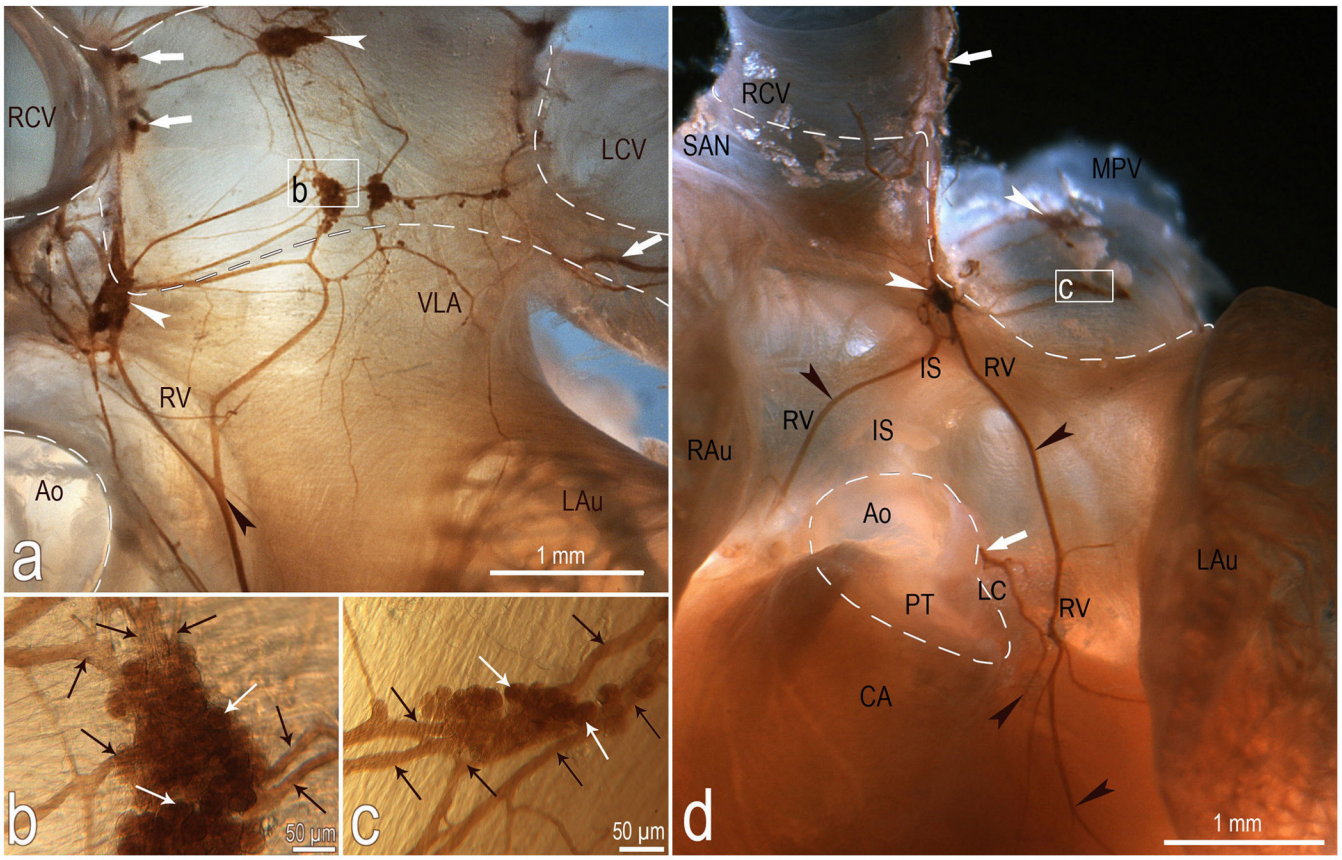

Fig 2.

Macrophotographs to illustrate the location and morphologic pattern of the right ventral (a, d), ventral left atrial (a) and left coronary (d) nerve subplexuses in a mouse heart stained histochemically for AChE. Boxed areas in **a** and **d** were enlarged employing a contact microscope and shown as **b** and **c** insets. Note the right ganglia situated at the root of right cranial vein and the left ganglia on the cranial-dorsal aspect of left atrium. *Black arrowheads*, some cardiac nerves; *white arrowheads*, ganglia. W*hite solid arrows*, nerves accessing the heart hilum and originating the right ventral (RV) and left coronary (LC) neural subplexuses; *black thin arrows*, interganglionic nerves, *white thin arrows*, some neurons located inside ganglia. Dashed line shows the limits of heart hilum. *Abbreviations:* **Ao** – aorta; **CA** – conus arteriosus; **IS** – ventral interatrial groove; **LAu** – left auricle; **LCV** – left cranial vein; **MPV** – middle pulmonary vein; **PT** – pulmonary trunk; **RAu** – right auricle; **RCV** – right cranial vein; **SAN** – sinuatrial nodal zone; neural subplexuses: **RV** – right ventral; **LC** – left coronary, **VLA** – ventral left atrial.

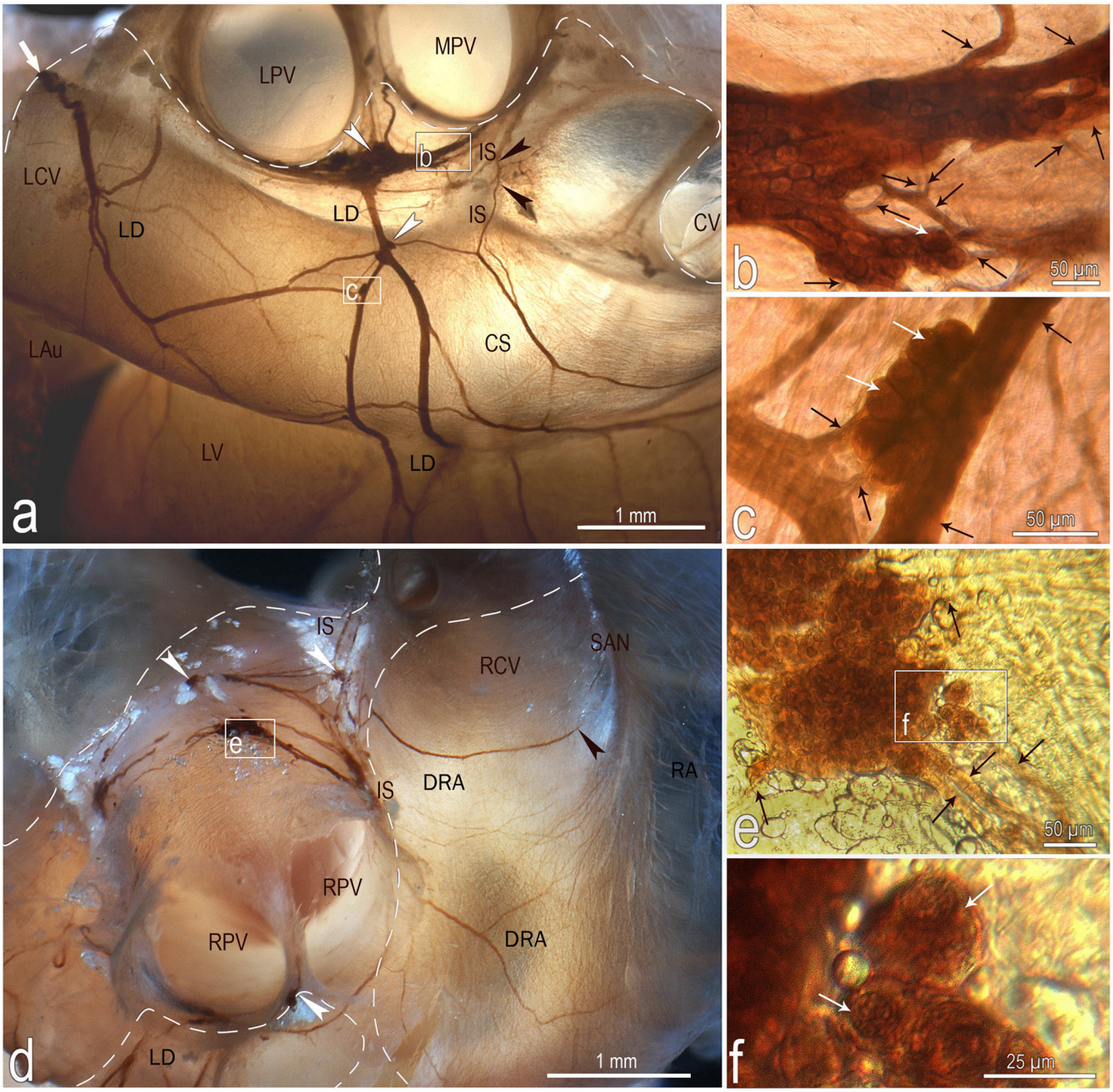

Fig 3.

Location, course and structure of left dorsal (LD) and dorsal right atrial (DRA) neural subplexuses in a mouse heart stained histochemically for acetylcholinesterase. Boxed areas b and c in a, e in d and f in e were enlarged using a contact microscope and shown respectively as b, c, e, and f insets. *Black arrowheads* in a point to the nerves that penetrate into interatrial septum, while in d one that proceeds toward the region of the sinuatrial node (SAN). W*hite arrowheads*, some ganglia; *white solid arrows*, nerves entering the ganglionated nerve plexus of the heart hilum; *Black thin arrows*, interganglionic nerves, *white thin arrows*, some neurons. Dashed line limits the heart hilum. In d, note the right ganglia situated at the root of right cranial vein on the interatrial groove. *Other*

a*bbreviations:* **CS** – coronary sinus; **CV** – orifice of caudal (inferior caval) vein; **IS** – interatrial groove; **LAu** – inferior surface of left auricle; **LCV** – left cranial vein; **LPV** – orifice of left pulmonary vein; **LV** – left ventricle; **RA** – right atrial wall; **MPV** – orifice of middle pulmonary vein; **RPV** – orifice of right pulmonary vein; **RCV** – root of right cranial (superior caval) vein.

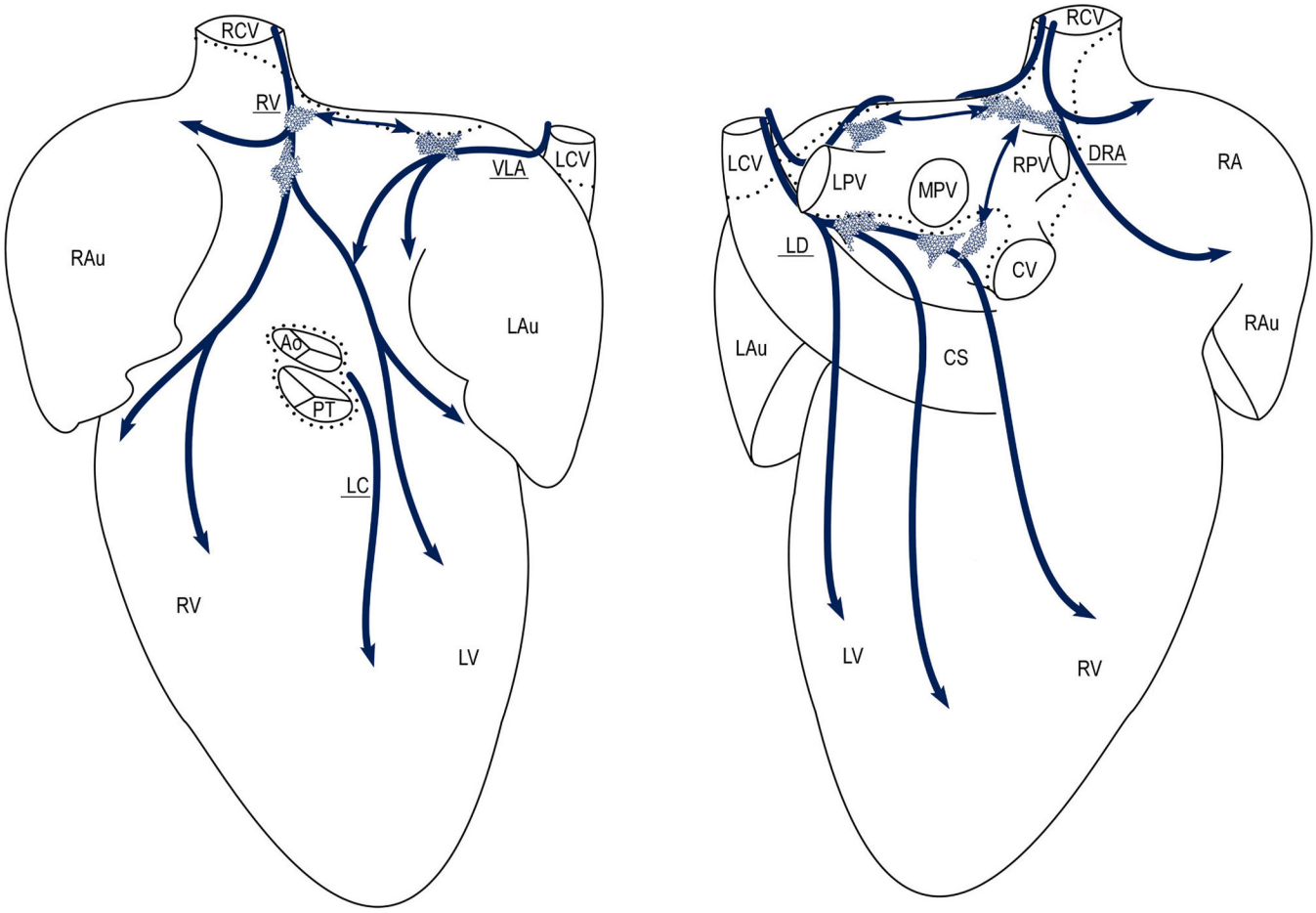

Fig 4.

Diagram summarizing the distribution and morphology of distinct intrinsic ganglionated nerve subplexuses in 15 mouse hearts as they were seen from the ventral (left) and dorsal (right) sides on a pressure-inflated heart stained histochemically for AChE. Dotted lines limit the heart hilum; thick arched arrows show the course of neural subplexuses; polygonal areas show the main locations of intrinsic ganglia in mouse heart. Note the left ganglia at the root of the left pulmonary vein and the right ganglia distributed above interatrial septum at the roots of right cranial (RCV) and middle pulmonary (MPV) veins. *Abbreviations*: **Ao** – aorta; **PT** – pulmonary trunk; **CS** – coronary sinus; veins: **CV** – caudal (inferior caval), **LCV** – left cranial (left azygos), **RCV** – right cranial (superior caval), **LPV** – left pulmonary, **RPV** – right pulmonary, and **MPV** – middle pulmonary; **LAu** – left auricle; **LV** – left ventricle; **RA** – right atrium; **RAu** – right auricle; **RV** – right ventricle; neural subplexuses: **VLA** – ventral left atrial, **DRA** – dorsal right atrial, **LC** – left coronary, **LD** – left dorsal, and **RV** – right ventral.

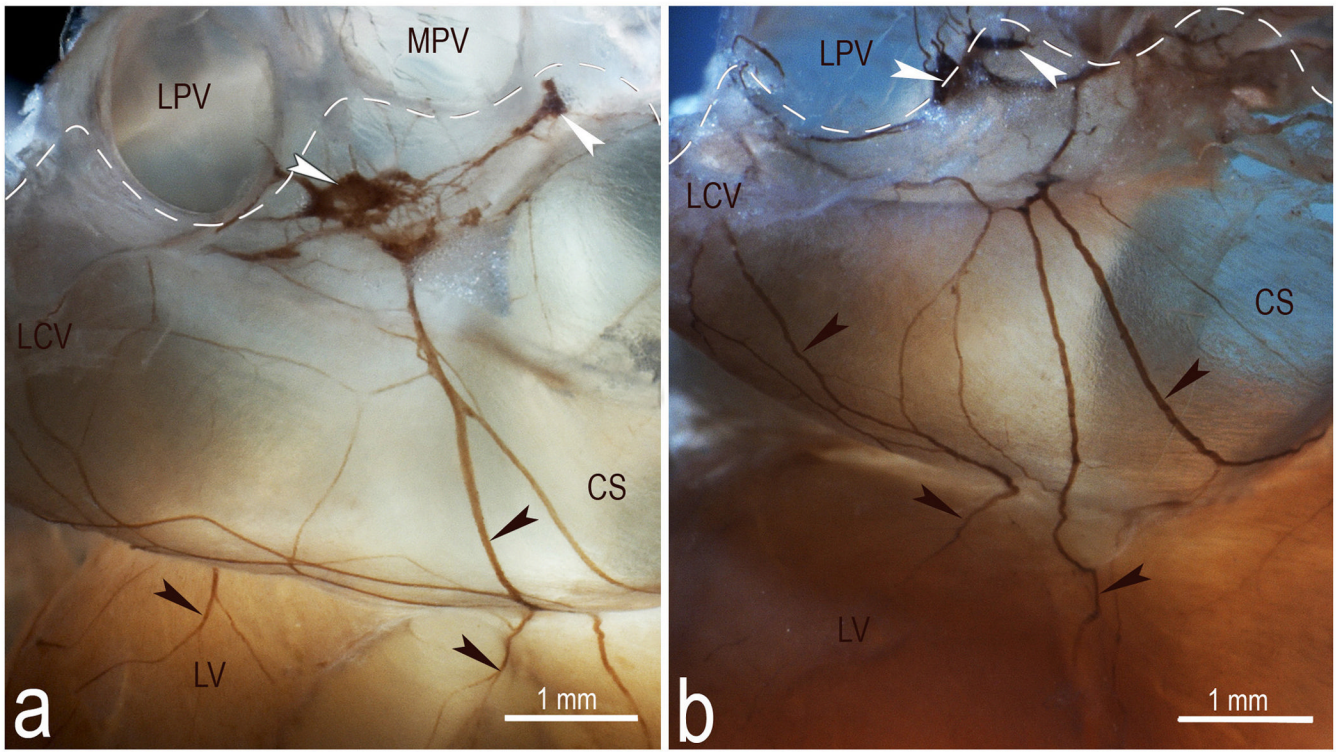

Fig 5.

Macrophotographs illustrating the structural variability of the left dorsal neural subplexus in two mouse hearts stained histochemically for AChE. *White arrowheads*, some ganglia, *black arrowheads*, topographically comparable nerves at coronary sinus. Dashed lines demarcate the limits of heart hilum. *Abbreviations*: **CS** – coronary sinus; **LCV** – left cranial (left azygos) vein; **LPV** – left pulmonary vein; **LV** – left ventricle; **MPV** – middle pulmonary vein. Note the persistent location of ganglia specified by white arrowheads.

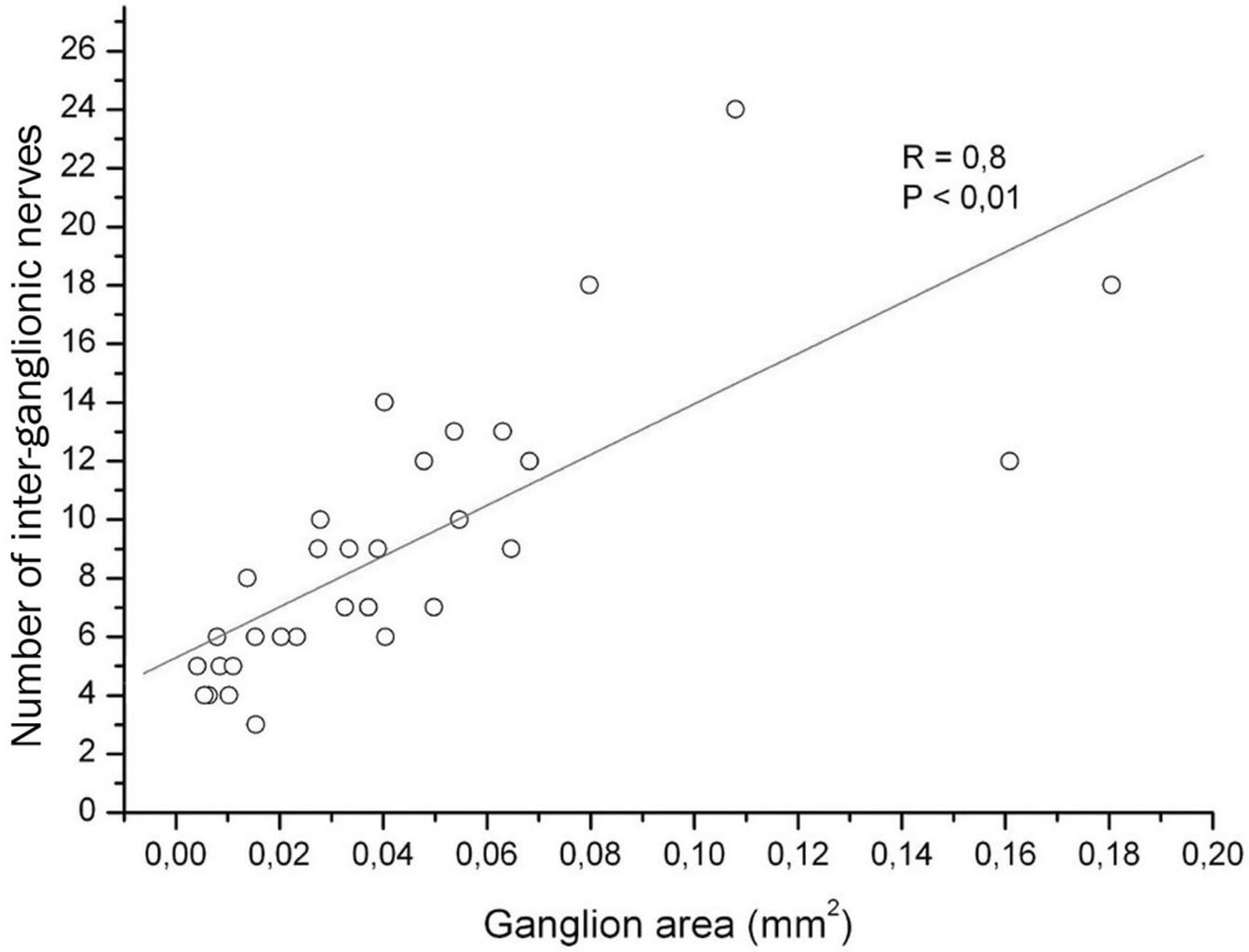

Fig 6.

The number of interganglionic nerves plotted against areas of 31 ganglia that were derived from ten mouse hearts. The straight line indicates the linear regression of the plotted data. Each point corresponds to one of the analyzed ganglion. *R*, correlation coefficient at $P < 0,05$.

Table 1

The number of intrinsic ganglia, their sizes, cumulative areas and the number inter-ganglionic nerves in 10 mouse hearts stained histochemically for AChE

Parameter	Mean	Range
Ganglion number per heart	19 ± 3	11 – 30
Ganglion size (in mm^2)	0,026 ± 0,003	0,001 – 0,167
Cumulative ganglion area (in mm^2)	0,35 ± 0,05	0,19 – 0,63
Number of inter-ganglionic nerves per ganglion	9 ± 1	3 – 24